arXiv:1412.2553v2 [cond-mat.soft] 19 Jan 2015

Conformational properties of complex polymers: rosette versus star-like structures

V. Blavatska

Institute for Condensed Matter Physics of the National Academy of Sciences of Ukraine, 79011 Lviv, Ukraine

E-mail: viktoria@icmp.lviv.ua

R. Metzler

Institute for Physics and Astronomy, University of Potsdam, 14476 Potsdam-Golm, Germany
Department of Physics, Tampere University of Technology, FI-33101 Tampere, Finland

Abstract. Multiple loop formation in polymer macromolecules is an important feature of the chromatin organisation and DNA compactification in the nuclei. We analyse the size and shape characteristics of complex polymer structures, containing in general f_1 loops (petals) and f_2 linear chains (branches). Within the frames of continuous model of Gaussian macromolecule, we apply the path integration method and obtain the estimates for gyration radius R_g and asphericity $\hat{A}$ of typical conformation as functions of parameters f_1, f_2. In particular, our results qualitatively reveal the extent of anisotropy of star-like topologies as compared to the rosette structures of the same total molecular weight.

PACS numbers: 36.20.Fz, 33.15.Bh, 87.15.hp

Submitted to: *J. Phys. A: Math. Gen.*

1. Introduction

Loop formation in macromolecules plays an important role in a number of biochemical processes: stabilisation of globular proteins [1–4], transcriptional regularisation of genes [5–7] as well as DNA compactification in the nucleus [8–10]. The localisation of chromatin fibres to semi-compact regions known as chromosome territories is maintained among others by the topological constraints introduced by multiple loops in chromatin organisation [11]. Numerous analytical and numerical studies have been conducted to analyse the cyclisation probability and loop size distributions in long flexible macromolecules [12–19]. The conformational properties of isolated loops (ring polymers) [20–32] and multiple loops [10, 33] have been intensively studied as well.

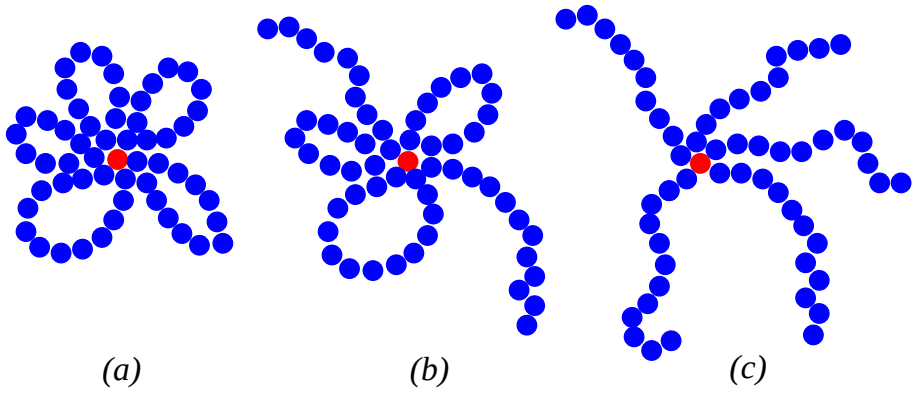

Figure 1. Schematic presentation of polymer systems of complex topologies.

Interlocking and entanglements are ubiquitous features of flexible polymers of high molecular weight. In particular, DNA can exist in the form of catenated (bonded) rings of various complexities [34–36]. The segments of different DNA molecules can intercross through the transient breaks introduced by special enzymes (topoisomerases) [37–39]. Numerous studies [40–47] reveal the advantage of linking in stabilisation of peptide and protein oligomers.

In this concern, it is worthwhile to study the conformational properties of generalised complex polymer structures, containing f_1 loops and f_2 linear chains of the same length S(see Fig. 1). The properties of so-called "rosette" (Fig. 1a) and "ring-linear" (Fig. 1b) structures have been considered recently in numerical simulations in Refs. [11,48]. However, only the shape properties of very simple structures of two bonded rings ($f_2 = 2, f_1 = 0$) and rings with two connected linear branches ($f_2 = 1, f_1 = 2$) with excluded volume effects were analysed [48]. In particular, a quite subtle difference in the conformational properties of two connected polymer rings compared with that of one isolated ring were found. On the other hand, the properties of "star" polymers (Fig. 1c) have been intensively studied by now [49–57].

In general, the statistics of polymers is known to be characterised by a set of universal properties, which are independent of the details of the microscopic chemical structure [58, 59]. In particular, the asymptotic number of possible conformations of structure shown in Fig. 1b obeys the scaling law [49]

$$\mathcal{Z}_{f_1 f_2} \sim \mu^{(f_1+f_2)S} S^{\gamma_{f_1 f_2}-1}, \;\; \gamma_{f_1 f_2} = 1 - d\nu f_1 + \sigma_{2f_1+f_2} + f_2\sigma_1. \tag{1}$$

Here, ν is the universal critical (Flory) exponent, governing the scaling of the size measure (e.g. the averaged gyration radius R_g) of macromolecule according to

$$\langle R^2_{g\, f_1 f_2}\rangle \sim ((f_1 + f_2)S)^{2\nu}, \tag{2}$$

σ_i is the set of so-called vertex exponents (with $\sigma_2 = 0$), d is the spatial dimension and μ is a non-universal fugacity. For an idealised Gaussian (phantom) macromolecule without any interactions between monomers one finds: $\nu = 1/2$, $\sigma_i = 0$. In the limiting cases ($f_1 = 0$) and ($f_2 = 0$), respectively, we obtain the corresponding critical exponents,

governing the scaling of the number of possible conformations of f_2-branch star and f_1-petal rosette polymers: $\gamma_{\rm star} = 1$, $\gamma_{\rm rosette} = 1 - df_1/2$. Therefore, additional topological constraints in rosette polymers lead to a considerable reduction of the number of allowed conformations, as compared with star polymers of the same molecular weight.

To compare the size measures of macromolecules of different topologies but of the same total molecular weight one can consider the universal size ratios. In particular, in the idealised Gaussian case, the ratio of the gyration radii of the individual ring and open linear structures reads [60]

$$\frac{\langle R^2_{g\,\rm ring}\rangle}{\langle R^2_{g\,\rm linear}\rangle} = \frac{1}{2}, \tag{3}$$

whereas comparing the size of f-branch star and a linear chain of the same total length one has [60]

$$\frac{\langle R^2_{g\,f\rm star}\rangle}{\langle R^2_{g\,\rm linear}\rangle} = \frac{3f-2}{f^2}. \tag{4}$$

Taking into account the excluded volume effect leads to an increase of this values [51, 61–66].

The overall shape of a typical polymer conformation is of great importance, affecting in particular the mobility and folding dynamics of proteins [67, 68]. The shape of DNA may be relevant for the accessibility for enzymes depending on the spatial distance between DNA-segments [69]. Already in 1934 it was realised [70] that the shape of a typical flexible polymer coil in a solvent is anisotropic and resembles that of a prolate ellipsoid. It is convenient to characterise the asymmetry of polymer configurations in terms of rotationally invariant universal quantities [71,72] constructed as combinations of the components of the gyration tensor, such as the asphericity $\hat{A}$. This quantity takes on a maximum value of unity for a completely stretched, rod-like configuration, and equals zero for the spherical form, thus obeying the inequality $0 \leq \hat{A} \leq 1$. In the Gaussian case, for the individual linear and circular polymer chains one has correspondingly [72]

$$\hat{A}_{\rm linear} = \frac{2(d+2)}{5d+4}, \tag{5}$$

$$\hat{A}_{\rm ring} = \frac{d+2}{5d+2}. \tag{6}$$

whereas the asphericity of f-branch star polymer reads [73]:

$$\hat{A}_{\rm star} = 2\frac{(2+d)(15f-14)}{5d(3f-2)^2+4(15f-14)}. \tag{7}$$

Note that Eq. (5) gives the asphericity of a trajectory of diffusive randomly walking particle. The influence of excluded volume effects on the shape parameters of single linear and ring polymers, as well as star polymers have been analysed so far both analytically [22, 71, 74] and numerically [75–79].

In the present paper, we study the universal size and shape characteristics of complex polymer structures (Fig. 1), applying the path integration method. A special

attention is paid to the analytical study of statistical properties of rosette (Fig. 1a) and ring-linear (Fig. 1b) structures.

The layout of the paper is as follows. In section 2, we shortly describe the presentation of complex polymer system within the frames of continuous chain model. Our results are given in Section 3. We end up by giving conclusions in Section 4.

2. The model

We consider a system consisting of f_1 closed polymer loops (petals) and f_2 linear chains (branches), all bonded together at one "branching" point (see Fig. 1b). Within the Edwards continuous chain model [80], each of the individual branches or petals is presented as a path of length S_i, parameterised by $\vec{r}_i(s)$, where s is varying from 0 to S_i $(i = 1, 2, \ldots, f_1 + f_2)$. For simplicity we take: $S_1 = \ldots = S_{f_1+f_2} = S$. The weight of the individual ith path is given by

$$W_i = \exp\left(-\frac{1}{2}\int_0^S \left(\frac{d\vec{r}_i(s)}{ds}\right)^2 ds\right) \tag{8}$$

and the partition function of the system can thus be written as

$$\mathcal{Z}_{f_1 f_2} = \frac{\displaystyle\int \mathcal{D}\vec{r} \prod_{j=1}^{f_1} \delta(\vec{r}_j(S) - \vec{r}_j(0)) \prod_{i=1}^{f_1+f_2} \delta(\vec{r}_i(0)) W_i}{\displaystyle\int \mathcal{D}\vec{r} \prod_{i=1}^{f_1+f_2} \delta(\vec{r}_i(0)) W_i}. \tag{9}$$

Here, $\int \mathcal{D}\vec{r}$ denotes functional path integrations over $f_1 + f_2$ trajectories. The products of δ-functions describe the fact that f_1 trajectories are closed and that the starting point of all trajectories is fixed (the "branching" point). Note, that (9) is normalised in such a way that the partition function of the system consisting of $f_1 + f_2$ open linear Gaussian chains (star-like structure) is unity.

Exploiting the Fourier-transform of the δ-functions

$$\delta(\vec{r}_j(S) - \vec{r}_j(0)) = (2\pi)^{-d} \int \mathrm{d}\vec{q}_j \, \mathrm{e}^{-i\vec{q}_j(\vec{r}_j(S) - \vec{r}_j(0))} \tag{10}$$

and rewriting in the exponent

$$-\frac{1}{2}\int_0^S \left(\frac{\mathrm{d}\vec{r}_j(s)}{\mathrm{d}s}\right)^2 \mathrm{d}s - i\vec{q}_j \int_0^S \frac{d\vec{r}_j(s)}{d\,s}\mathrm{d}s = -\frac{1}{2}\int_0^S \mathrm{d}s \left(\left(\frac{\mathrm{d}\vec{r}_j(s)}{\mathrm{d}s} + i\vec{q}_j\right)^2 + q^2\right)$$

we evaluate the expression of partition function (9), giving the asymptotic number of possible conformations of polymer system

$$\mathcal{Z}_{f_1 f_2} = (2\pi)^{-f_1 d} \prod_{j=1}^{f_1} \int \mathrm{d}\vec{q}_j \, \mathrm{e}^{-\frac{q_j^2 S}{2}} = (2\pi S)^{-df_1/2}. \tag{11}$$

Comparing this relation with Eq. (1), we recover the estimate for the critical exponent $\gamma_{f_1 f_2} = 1 - df_1/2$.

The average of any observable $\langle(\ldots)\rangle$ over an ensemble of conformations is then given by:

$$\langle(\ldots)\rangle = \frac{1}{\mathcal{Z}_{f_1 f_2}} \frac{\displaystyle\int \mathcal{D}\vec{r} \prod_{j=1}^{f_1} \delta(\vec{r}_j(S) - \vec{r}_j(0)) \prod_{i=1}^{f_1+f_2} \delta(\vec{r}_i(0))(\ldots) W_i}{\displaystyle\int \mathcal{D}\vec{r} \prod_{i=1}^{f_1+f_2} \delta(\vec{r}_i(0)) W_i}. \tag{12}$$

3. Size ratios and asphericity

The size and shape characteristics of a typical polymer conformation can be characterised [79] in terms of the gyration tensor $\mathbf{Q}$. Within the framework of a continuous polymer model the components of this tensor can be presented as

$$Q_{\alpha\beta} = \frac{1}{2S^2(f_1+f_2)^2} \sum_{i,j=1}^{f_1+f_2} \int_0^S ds_1 \int_0^S ds_2 \; (\vec{r}_i^{\,\alpha}(s_2) - \vec{r}_j^{\,\alpha}(s_1))(\vec{r}_i^{\,\beta}(s_2) - \vec{r}_j^{\,\beta}(s_1)), \tag{13}$$

where $r_i^\alpha(s_1)$ is αth component of $\vec{r}_i(s_1)$ ($\alpha = 1, 2, \ldots, d$).

For the averaged radius of gyration one has

$$\langle R^2_{g\, f_1 f_2}\rangle = \frac{1}{2S^2(f_1+f_2)^2} \sum_{i,j=1}^{f_1+f_2} \left\langle \int_0^S ds_1 \int_0^{s_1} ds_2 (\vec{r}_i(s_2) - \vec{r}_j(s_1))^2 \right\rangle \tag{14}$$

$$= \langle \mathrm{Tr}\, \mathbf{Q}\rangle.$$

Here and below, $\langle(\ldots)\rangle$ denotes averaging over an ensemble of path conformations according to (12).

The spread in the eigenvalues λ_i of the gyration tensor (13) describes the distribution of monomers inside the polymer coil and thus measures the asymmetry of the molecule. For a symmetric (spherical) configuration all the eigenvalues λ_i are equal, whereas for completely stretched rod-like conformation all λ_i are zero except one. Let $\overline{\lambda} \equiv \mathrm{Tr}\, \mathbf{Q}/d$ be the mean eigenvalue of the gyration tensor. Then one may characterise the extent of asphericity of a macromolecule by the quantity $\hat{A}$ defined as [71]:

$$\hat{A} = \frac{1}{d(d-1)} \sum_{i=1}^{d} \frac{\langle(\lambda_i - \overline{\lambda})^2\rangle}{\langle \overline{\lambda}^2\rangle} = \frac{d}{d-1} \frac{\langle \mathrm{Tr}\, \hat{\mathbf{Q}}^{\mathbf{2}}\rangle}{\langle(\mathrm{Tr}\, \mathbf{Q})^2\rangle}, \tag{15}$$

with $\hat{\mathbf{Q}} \equiv \mathbf{Q} - \overline{\lambda}\, \mathbf{I}$ (here $\mathbf{I}$ is the unity matrix). This universal quantity equals zero when $\lambda_i = \overline{\lambda}$, and takes a maximum value of one in the case of a rod-like configuration. The asphericity (15) can be rewritten in terms of the averaged components of gyration tensor (13) as follows [71]:

$$\hat{A} = \frac{\langle Q_{\alpha\alpha} Q_{\alpha\alpha}\rangle + d\langle Q_{\alpha\beta} Q_{\alpha\beta}\rangle - \langle Q_{\alpha\alpha} Q_{\beta\beta}\rangle}{\langle Q^2_{\alpha\alpha}\rangle + (d-1)\langle Q_{\alpha\alpha} Q_{\beta\beta}\rangle}. \tag{16}$$

Below, we give detailed evaluation of the expressions for the averaged radius of gyration (14) and asphericity (16) of the model (9) within the framework of path integration approach.

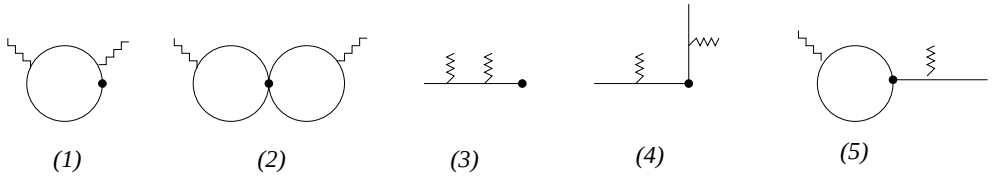

Figure 2. Diagrammatic presentation of contributions into $\langle\xi(\vec{k})\rangle$. The solid line on a diagram is a schematic presentation of a polymer path of length S, and wavy lines denote so-called restriction points s_1 and s_2. With $\bullet$ we denote the position of the starting "branching" point.

3.1. Radius of gyration

The radius of gyration (14) can be calculated from the identity

$$(\vec{r}_i(s_2)-\vec{r}_j(s_1))^2=-2\mathrm{d}\frac{\partial}{\partial|k|^2}\xi(\vec{k})\Big|_{k=0},\ \ \xi(\vec{k})\equiv \mathrm{e}^{i\vec{k}\vec{r}_i(s_2)-\vec{r}_j(s_1)}, \tag{17}$$

and evaluating $\langle\xi(\vec{k})\rangle$ in the path integration approach. In calculation of the contributions into $\langle\xi(\vec{k})\rangle$ it is convenient to use the diagrammatic presentation as given in Fig. 2. According to the general rules of diagram calculations [59], each segment between any two restriction points s_a and s_b is oriented and bears a wave vector $\vec{q}_{ab}$ given by a sum of incoming and outcoming wave vectors injected at restriction points and end points. At these points, the flow of wave vectors is conserved. A factor $\exp\left(-\vec{q}_{ab}^{\,2}(s_b-s_a)/2\right)$ is associated with each segment. An integration is to be made over all independent segment areas and over wave vectors injected at the end points.

The analytic expressions, corresponding to the diagrams (1)-(5) in Fig. 2 then read

$$\begin{aligned}
\langle\xi(\vec{k})\rangle_{(1)} &= \left(\frac{S}{2\pi}\right)^{\frac{d}{2}}\mathrm{e}^{-\frac{k^2}{2}(s_2-s_1)}\int \mathrm{d}q_1\,\mathrm{e}^{-\frac{{q_1}^2}{2}S}\mathrm{e}^{-kq_1(s_2-s_1)} = \\
&= \mathrm{e}^{-\frac{k^2}{2}\frac{(s_2-s_1)(S-s_2+s_1)}{S}}, && (18)\\
\langle\xi(\vec{k})\rangle_{(2)} &= \left(\frac{S}{2\pi}\right)^{d}\mathrm{e}^{-\frac{k^2}{2}(s_2+s_1)}\int \mathrm{d}q_1\int \mathrm{d}q_2\,\mathrm{e}^{-\frac{{q_1}^2}{2}S}\mathrm{e}^{-\frac{{q_2}^2}{2}S}\mathrm{e}^{-q_1ks_1}\mathrm{e}^{-q_2ks_2} = \\
&= \mathrm{e}^{-\frac{k^2}{2}\frac{S(s_1+s_2)-s_1^2-s_2^2}{S}}, && (19)\\
\langle\xi(\vec{k})\rangle_{(3)} &= \mathrm{e}^{-\frac{k^2}{2}(s_2-s_1)}, && (20)\\
\langle\xi(\vec{k})\rangle_{(4)} &= \mathrm{e}^{-\frac{k^2}{2}(s_2+s_1)}, && (21)\\
\langle\xi(\vec{k})\rangle_{(5)} &= \left(\frac{S}{2\pi}\right)^{\frac{d}{2}}\mathrm{e}^{-\frac{k^2}{2}(s_2+s_1)}\int \mathrm{d}q_1\,\mathrm{e}^{-\frac{{q_1}^2}{2}S}\mathrm{e}^{-kq_1s_1} = \mathrm{e}^{-\frac{k^2}{2}\frac{S(s_1+s_2)-s_1^2}{S}}. && (22)
\end{aligned}$$

Taking the derivatives with respect to k according to (17) in the expressions above and taking into account the combinatorial factors, we find for the radius of gyration

$$\begin{aligned}
\langle R^2_{g\,f_1f_2}\rangle = \frac{Sd}{(f_1+f_2)^2S^2}\Bigg(f_1\int_0^S ds_2\int_0^{s_2} ds_1\frac{(s_2-s_1)(S-s_2+s_1)}{S}+ \\
+\frac{f_1(f_1-1)}{2}\int_0^S ds_2\int_0^S ds_1\frac{(s_2-s_1)(S(s_1+s_2)-s_1^2-s_2^2)}{S}+
\end{aligned}$$

$$+ f_2 \int_0^S ds_2 \int_0^{s_2} ds_1 (s_2 - s_1) + \frac{f_2(f_2-1)}{2} \int_0^S ds_2 \int_0^S ds_1 (s_2 + s_1) +$$
$$+ f_1 f_2 \int_0^S ds_2 \int_0^S \frac{(s_2 - s_1)(S(s1 + s_2) - s_1^2)}{S} \Bigg) =$$
$$= \frac{Sd}{(f_1+f_2)^2} \frac{1}{12} \left[f_1(2f_1 - 1) + 2f_2(3f_2 - 2) + 8f_1 f_2 \right]. \tag{23}$$

The case $f_2 = 0$ corresponds to the rosette structure (Fig. 1a) with

$$\langle R^2_{g\,\mathrm{rosette}} \rangle = \frac{Sd}{12 f_1}(2f_1 - 1), \tag{24}$$

at $f_1 = 1$ one recovers the gyration radius of individual ring polymer. The case $f_1 = 0$ corresponds to star structure (Fig. 1c) with

$$\langle R^2_{g\,\mathrm{star}} \rangle = \frac{Sd}{6 f_2}(3f_2 - 2), \tag{25}$$

at $f_2 = 1$ one receives the gyration radius of linear polymer chain.

For the size ratio of rosette and star polymers of the same total molecular weight (corresponding to $f_1 = f_2 = f$) we obtain

$$g \equiv \frac{\langle R^2_{g\,\mathrm{rosette}} \rangle}{\langle R^2_{g\,\mathrm{star}} \rangle} = \frac{1}{2} \frac{2f - 1}{3f - 2}. \tag{26}$$

Note that putting $f = 1$ in above relation, one restores the size ratio of the ring and open linear chain of the same molecular weight (3). The quantity (26) decreases with increasing the branching parameter f and in the limit $f \to \infty$ reaches the asymptotic value 1/3 (see Fig. 3).

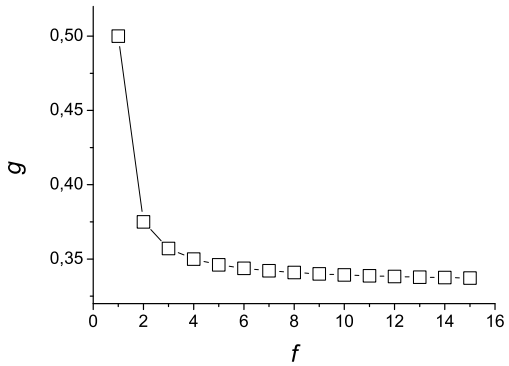

Figure 3. Size ratio (26) of rosette and star polymers of the same total molecular weight as function of branching parameter f. Line is guide to the eyes.

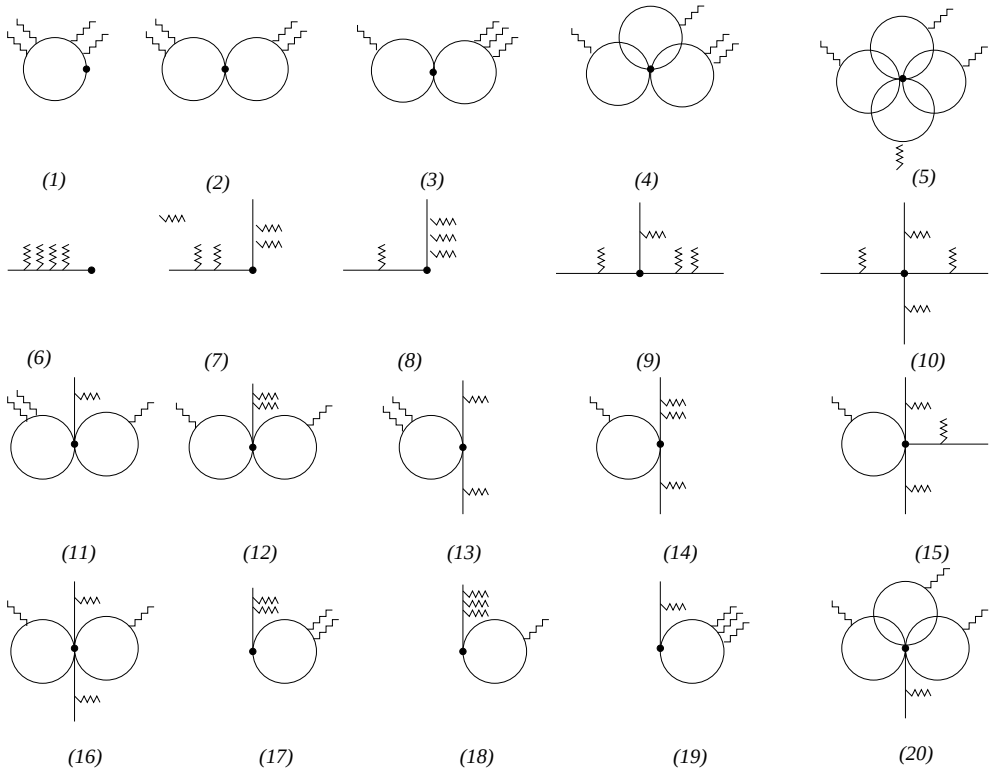

Figure 4. Diagrammatic presentation of contributions into $\langle\zeta(\vec{k}_1,\vec{k}_2)\rangle$. The wavy lines denote restriction points s_1, s_2, s_3, s_4. With $\bullet$ we denote the position of the starting "branching" point.

3.2. Asphericity

The products of the components of the gyration tensor (13) which appear in (16) can be calculated using the identity

$$(\vec{r}_i^{\,\alpha}(s_2)-\vec{r}_j^{\,\alpha}(s_1))(\vec{r}_i^{\,\beta}(s_2)-\vec{r}_j^{\,\beta}(s_1))(\vec{r}_l^{\,\alpha}(s_4)-\vec{r}_m^{\,\alpha}(s_3))(\vec{r}_l^{\,\beta}(s_4)-\vec{r}_m^{\,\beta}(s_3)) =$$
$$= \frac{d}{dk_1^\alpha}\frac{d}{dk_1^\beta}\frac{d}{dk_2^\alpha}\frac{d}{dk_2^\beta}\,\zeta(\vec{k}_1,\vec{k}_2)\Big|_{\vec{k}_1=\vec{k}_2=0} \tag{27}$$

with

$$\zeta(\vec{k}_1,\vec{k}_2) = \mathrm{e}^{-\vec{k}_1(\vec{r}_i(s_2)-\vec{r}_j(s_1))}\mathrm{e}^{-\vec{k}_2(\vec{r}_l(s_4)-\vec{r}_m(s_3))}. \tag{28}$$

Again, we will use the diagrammatic presentation of contributions into $\langle\zeta(\vec{k}_1,\vec{k}_2)\rangle$ (see Fig. 4). Applying the same rules of diagram calculation, as introduced in the previous subsection and evaluating the corresponding expressions we find

$$\langle Q_{\alpha\beta}Q_{\alpha\beta}\rangle = f_1 D^{(1)}_{\alpha\beta|\alpha\beta} + \frac{f_1(f_1-1)}{2}(D^{(2)}_{\alpha\beta|\alpha\beta} + D^{(3)}_{\alpha\beta|\alpha\beta}) +$$
$$+\frac{f_1(f_1-1)(f_1-2)}{6}D^{(4)}_{\alpha\beta|\alpha\beta} + \frac{f_1(f_1-1)(f_1-2)(f_1-3)}{24}D^{(5)}_{\alpha\beta|\alpha\beta} +$$
$$+f_2 D^{(6)}_{\alpha\beta|\alpha\beta} + \frac{f_2(f_2-1)}{2}(D^{(7)}_{\alpha\beta|\alpha\beta} + D^{(8)}_{\alpha\beta|\alpha\beta}) +$$

$$+\frac{f_2(f_2-1)(f_2-2)}{6}D^{(9)}_{\alpha\beta|\alpha\beta}+\frac{f_2(f_2-1)(f_2-2)(f_2-3)}{24}D^{(10)}_{\alpha\beta|\alpha\beta}+$$
$$+\frac{f_1(f_1-1)f_2}{2}(D^{(11)}_{\alpha\beta|\alpha\beta}+D^{(12)}_{\alpha\beta|\alpha\beta})++\frac{f_1f_2(f_2-1)}{2}(D^{(13)}_{\alpha\beta|\alpha\beta}+D^{(14)}_{\alpha\beta|\alpha\beta})+$$
$$+\frac{f_1f_2(f_2-1)(f_2-2)}{6}D^{(15)}_{\alpha\beta|\alpha\beta}+\frac{f_1(f_1-1)f_2(f_2-2)}{4}D^{(16)}_{\alpha\beta|\alpha\beta}+$$
$$+f_1f_2(D^{(17)}_{\alpha\beta|\alpha\beta}+D^{(18)}_{\alpha\beta|\alpha\beta}+D^{(19)}_{\alpha\beta|\alpha\beta})+\frac{f_1(f_1-1)(f_1-2)f_2}{6}D^{(20)}_{\alpha\beta|\alpha\beta}. \qquad (29)$$

Here, $D^{(n)}_{\alpha\beta|\alpha\beta}$ denotes contribution of nth diagram on Fig. 4 (see Appendix for details).

The resulting expression for the asphericity thus reads

$$\hat{A}_{f_1f_2}=(2+d)\left[8f_2^2(15f_2-14)+f_1^2(8f_1-7)+\right.$$
$$+4f_1f_2(62f_1+28f_2-41)]\times\left[5d\left(4f_2^2(3f_2-2)^2+f_1^2(2f_1+1)^2+\right.\right.$$
$$\left.+4f_1f_2(f_2^2(72f_2-238)-f_1^2(24f_1+113)+196)\right)+2f_1^2(8f_1-7)+$$
$$\left.+16f_2^2(15f_2-14)+8f_1f_2(62f_1+34f_2-41)\right]^{-1}. \qquad (30)$$

The case $f_2=0$ corresponds to the rosette structure (Fig. 1a) with

$$\hat{A}_{\rm rosette}=\frac{(2+d)(8f_1-7)}{5d(2f_1-1)^2+2(8f_1-7)}, \qquad (31)$$

at $f_1=1$ one restores the expression of the asphericity of an individual ring polymer (6). Note that for the system of two bonded rings ($f_2=2$) we restore expression (6) in accordance with the numerical results of Ref. [48]. The case $f_1=0$ corresponds to star

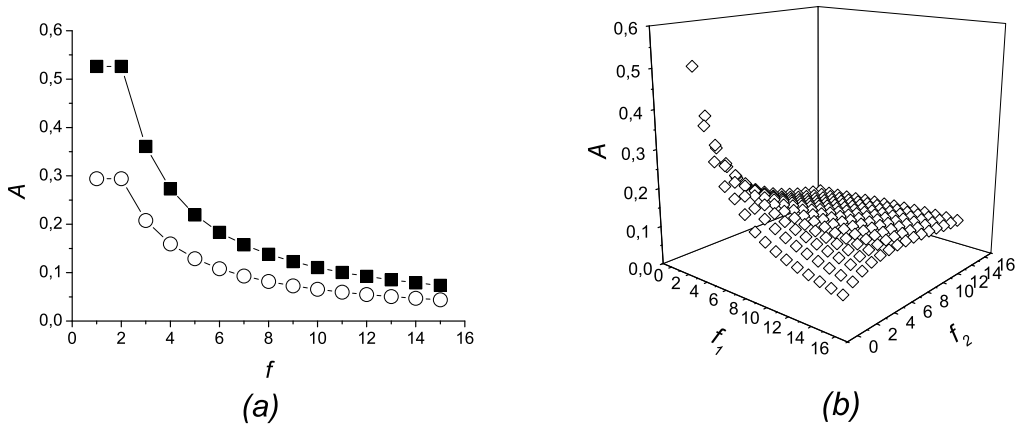

Figure 5. (a): Asphericity of rosette structure (31) (open circles) and star-like structure (32) (filled squares) of the same total molecular weight as functions of branching parameter f in space dimension $d=3$. Lines are guides to the eyes. (b): Asphericity of the system consisting of f_1 polymer loops and f_2 linear branches (30) as function of f_1, f_2 in space dimension $d=3$.

structure (Fig. 1c) with

$$\hat{A}_{\rm star} = 2\frac{(2+d)(15f_2-14)}{5d(3f_2-2)^2+4(15f_2-14)}. \qquad (32)$$

Again, at $f_2 = 1,\ 2$ one restores an expression of asphericity of an individual linear polymer (5).

To compare the degree of asphericity of rosette and star polymer structures of the same molecular weight (at $f_1 = f_2 = f$), we plot the above given quantities as functions of f at fixed $d = 3$ (see Fig. 5a). At small f, the star polymers are more anisotropic and extended in space than rosette structures, whereas both $\hat{A}_{\rm star}$ and $\hat{A}_{\rm rosette}$ gradually tend to zero with increasing f. Really, in the asymptotic limit $f \to \infty$ both the rosette and star structures can be treated as soft colloidal particles with highly symmetrical shape. The total asphericity of the system consisting of f_1 closed polymer loops and f_2 linear branches (Eq. (30)) is plotted as function of $f_1,\ f_2$ at fixed $d = 3$ in Fig. 5b. The value of this quantity is the result of competition of two effects: decreasing the asymmetry with increasing the number of closed loops and increasing the degree of anisotropy with increasing the number of linear branches.

4. Conclusions

In the present paper, we analysed the conformational properties of polymer systems of complex topologies (see Fig. 1). Whereas the properties of so-called star polymers (Fig. 1c) have been intensively studied, much less is known about the details of rosette (Fig. 1a) and ring-linear (Fig. 1b) structures. Multiple loop formation in polymer macromolecules plays an important role in biochemical processes such as DNA compactification [8–10], which makes the rosette-like structures interesting objects to study. Note, that another possible interpretation of structures (Fig. 1a) and (Fig. 1b) is the following: they can be treated as projections of long flexible polymer in the bulk onto the 2-dimensional plane [42].

Restricting ourselves to the idealised Gaussian case, when any interactions between monomers are neglected, we develop the continuous chain representation of the complex polymer model, considering each of the individual branches or petals as a path of length S_i, parameterised by $\vec{r}_i(s)$, where s is varying from 0 to S_i $(i = 1, 2, \ldots, f_1 + f_2)$. The size and shape characteristics of a typical polymer conformation have been studied on the basis of the gyration tensor $\mathbf{Q}$ with the the components given by (13). Working within the framework of path integration method and making use of appropriate diagram technique, we obtained the expressions for the gyration radius $\langle R^2_{g\,f_1 f_2}\rangle$ and asphericity $\hat{A}$, measuring the extent of anisotropy of a typical conformation of complex polymer structures, as functions of parameters $f_1,\ f_2$. In particular, our analytical results quantitatively confirm the compactification (decrease of the effective size) of multiple loop polymer structures as compared with structures containing linear segments [Eq. (26)]. A decrease of the anisotropy of rosette polymers as compared to star-like structures of the same total molecular weight is revealed, as well [Eqs. (31), (32)].

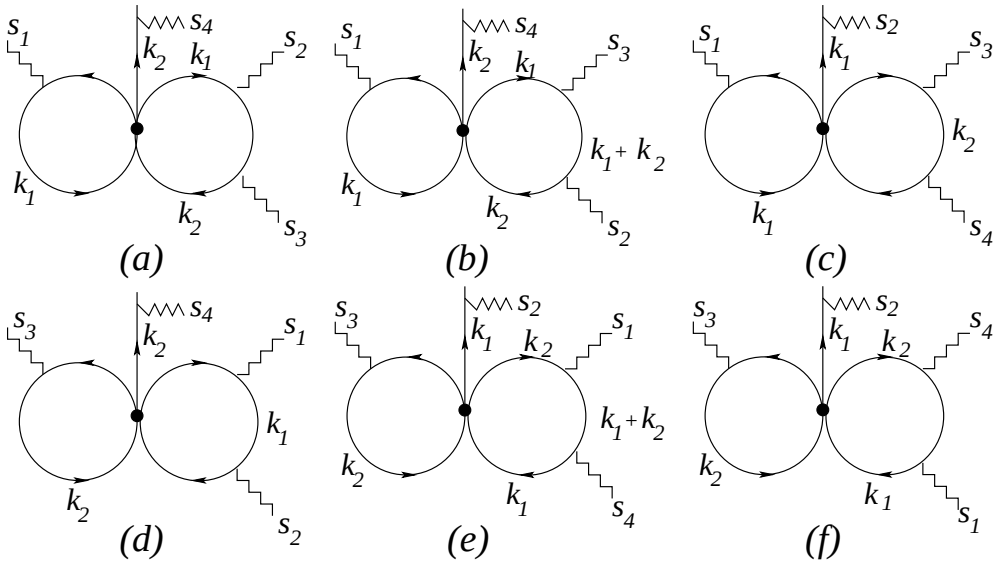

Figure 6. Diagram (11) on Fig. 4 with various permutations of restriction points s_1, s_2, s_3, s_4.

Acknowledgements

This work was supported by the FP7 EU IRSES projects N269139 "Dynamics and Cooperative Phenomena in Complex Physical and Biological Media" and N295302 "Statistical Physics in Diverse Realizations". Financial support from the Academy of Finland within the FiDiPro scheme is acknowledged.

Appendix

Here, we evaluate the analytical expressions, corresponding to diagram (11) on Fig. 4. Note, that in the diagram calculations one should take into account the possible permutations of positions of restriction points s_1, s_2, s_3, s_4 (see Fig. 6).

The resulting expressions read:

$$\zeta^{(11)a}(\vec{k}_1,\vec{k}_2) = \mathrm{e}^{-\frac{k_1^2}{2}(S-s_1+s_2)}\mathrm{e}^{-\frac{k_2^2}{2}(S-s_3+s_4)}\int\mathrm{d}q_1\int\mathrm{d}q_2\,\mathrm{e}^{-\frac{q_1^2}{2}S}\mathrm{e}^{-\frac{q_2^2}{2}S}\times$$
$$\times\mathrm{e}^{-q_1k_1(S-s_1)}\mathrm{e}^{-q_2k_1s_2}\mathrm{e}^{-q_2k_2(S-s_3)} =$$
$$= \mathrm{e}^{-\frac{k_1^2}{2S}(S(s_1+s_2)-s_1^2-s_2^2)-\frac{k_2^2}{2S}(S(s_3+s_4)-s_3^2)+\frac{k_1k_2}{S}s_2(S-s_3)},$$
$$\zeta^{(11)b} = \mathrm{e}^{-\frac{k_1^2}{2}(S-s_1+s_2)}\mathrm{e}^{-\frac{k_2^2}{2}(S-s_3+s_4)}\mathrm{e}^{-k_1k_2(s_2-s_3)}\int\mathrm{d}q_1\int\mathrm{d}q_2\,\mathrm{e}^{-\frac{q_1^2}{2}S}\mathrm{e}^{-\frac{q_2^2}{2}S}\times$$
$$\times\mathrm{e}^{-q_1k_1(S-s_1)}\mathrm{e}^{-q_2k_1s_2}\mathrm{e}^{-q_2k_2(S-s_3)} =$$
$$= \mathrm{e}^{-\frac{k_1^2}{2S}(S(s_1+s_2)-s_1^2-s_2^2)-\frac{k_2^2}{2S}(S(s_3+s_4)-s_3^2)+\frac{k_1k_2}{S}(s_2(S-s_3)-S(s_2-s_3))},$$
$$\zeta^{(11)c} = \mathrm{e}^{-\frac{k_1^2}{2}(S-s_1+s_2)}\mathrm{e}^{-\frac{k_2^2}{2}(s_4-s_3)}\int\mathrm{d}q_1\int\mathrm{d}q_2\,\mathrm{e}^{-\frac{q_1^2}{2}S}\mathrm{e}^{-\frac{q_2^2}{2}S}\mathrm{e}^{-q_1k_1(S-s_1)}\times$$
$$\times\mathrm{e}^{-q_2k_2(s_4-s_3)} = \mathrm{e}^{-\frac{k_1^2}{2}(s_1+s_2)-\frac{k_2^2}{2S}(s_4-s_3)(S-s_4+s_3)},$$

$$\zeta^{(11)d} = \mathrm{e}^{-\frac{k_1^2}{2}(s_2-s_1)}\mathrm{e}^{-\frac{k_2^2}{2}(S-s_3+s_4)}\int \mathrm{d}q_1 \int \mathrm{d}q_2\, \mathrm{e}^{-\frac{q_1^2}{2}S}\mathrm{e}^{-\frac{q_2^2}{2}S}\mathrm{e}^{-q_1k_2(S-s_3)} \times$$
$$\times \mathrm{e}^{-q_2k_1(s_2-s_1)} = \mathrm{e}^{-\frac{k_1^2}{2S}(s_2-s_1)(S-s_2+s_1)-\frac{k_2^2}{2}(s_3+s_4)},$$
$$\zeta^{(11)e} = \mathrm{e}^{-\frac{k_1^2}{2}(S-s_1+s_2)}\mathrm{e}^{-\frac{k_2^2}{2}(S-s_3+s_4)}\mathrm{e}^{-k_1k_2(s_4-s_1)}\int \mathrm{d}q_1 \int \mathrm{d}q_2\, \mathrm{e}^{-\frac{q_1^2}{2}S}\mathrm{e}^{-\frac{q_2^2}{2}S} \times$$
$$\times \mathrm{e}^{-q_1k_2(S-s_3)}\mathrm{e}^{-q_2k_1(S-s_1)}\mathrm{e}^{-q_2k_2s_4} =$$
$$= \mathrm{e}^{-\frac{k_1^2}{2S}(S(s_1+s_2)-s_1^2)-\frac{k_2^2}{2S}(S(s_3+s_4)-s_3^2-s_4^2)+\frac{k_1k_2}{S}(s_4(S-s_1)-S(s_4-s_1))},$$
$$\zeta^{(11)f} = \mathrm{e}^{-\frac{k_1^2}{2}(S-s_1+s_2)}\mathrm{e}^{-\frac{k_2^2}{2}(S-s_3+s_4)}\int \mathrm{d}q_1 \int \mathrm{d}q_2\, \mathrm{e}^{-\frac{q_1^2}{2}S}\mathrm{e}^{-\frac{q_2^2}{2}S}\mathrm{e}^{-q_1k_2(S-s_3)} \times$$
$$\times \mathrm{e}^{-q_2k_2s_4}\mathrm{e}^{-q_2k_1(S-s_1)} =$$
$$\mathrm{e}^{-\frac{k_1^2}{2S}(S(s_1+s_2)-s_1^2)-\frac{k_2^2}{2S}(S(s_3+s_4)-s_4^2)+\frac{k_1k_2}{S}s_4(S-s_1)}.$$

Taking derivatives over the components of k_1, k_2 in expressions above according to (27) and integrating over $s_1, \ldots, s_4$, one finally obtains the contributions $D^{(11)}_{\alpha\beta|\alpha\beta}$ in (29):

$$D^{(11)}_{\alpha\alpha|\alpha\alpha} = \frac{59}{45}S^6, \quad D^{(11)}_{\alpha\alpha|\beta\beta} = \frac{11}{9}S^6, \quad D^{(11)}_{\alpha\beta|\alpha\beta} = \frac{2}{45}S^6. \tag{33}$$

References

[1] L.J. Perry and R. Wetzel, Science **226**, 555 (1984).
[2] J.A. Wells and D.B. Powers, J. Biol. Chem. **261**, 6564 (1986).
[3] C.N. Pace, G.R. Grimsley, J.A. Thomson, and B.J. Barnett, J. Biol. Chem. **263**, 11820 (1988).
[4] A.D. Nagi and L. Regan, Folding Des. **2**, 67 (1997).
[5] R. Schlief, Science **240**, 127 (1988).
[6] K. Rippe, P.H. von Hippel, and J. Langowski, Trends. Biochem. Sci. **20**, 500 (1995).
[7] K. B. Towles, J.F. Beausang, H.G. Garcia, R. Phillips, and P.C. Nelson, Phys. Biol. **6**, 025001 (2009).
[8] P. Fraser, Curr. Opin. Genet. Dev. **16**, 490 (2006)
[9] M. Simonis, P. Klous, E. Splinter, Y. Moshkin, R. Willemsen, E. de Wit, B. van Steensel, and W. de Laat, Nat. Genet. **38**, 1348 (2006).
[10] J. Dorier and A. Stasiak, Nucl. Acids Res. **37**, 6316 (2009).
[11] S. de Nooijer, J. Wellink, B. Mulder, and T. Bisseling, Nucl. Acids Res. **37**, 3558 (2009).
[12] H.S. Chan and K.A. Dill, J. Chem. Phys. **90**, 492 (1989).
[13] A. Rey and J.J. Freire, Macromolecules **24**, 4673 (1991).
[14] A.M. Rubio, J.J. Freire, M. Bishop, and J.H.R. Clarke, Macromolecules **26**, 4018 (1993).
[15] M. Wittkop, S. Kreitmeier, and D. Göritz, J. Chem. Phys **104**, 351 (1996).
[16] H.-X. Zhou, J. Phys. Chem. **104**, 6763 (2001).
[17] T. Cui, J. Ding, and J.Z.Y. Chen, Macromolecules **39**, 5540 (2006).
[18] N.N. Toan, D. Marenduzzo, P.R. Cook, and C. Micheletti, Phys. Rev. Lett. **97**, 178302 (2006).
[19] J. Shin, A. G. Cherstvy, and R. Metzler, Soft Matter DOI: 10.1039/C4SM02007C
[20] M. Bishop and C. Saltiel, J. Chem. Phys. **85**, 6728 (1986).
[21] H.W. Diehl and E. Eisenriegler, J. Phys. A: Math. Gen. **22**, L87 (1989).
[22] O. Jagodzinski, E. Eisenriegler, and K. Kremer, J. Phys. I France **2**, 2243 (1992).
[23] S.P. Obukhov, M. Rubinstein, and T. Duke, Phys. Rev. Lett. **73**, 1263 (1994).
[24] M. Muller, J.P. Wittmer, and M.E. Cates, Phys.Rev.E **61**, 4078 (2000).
[25] J.M. Deutsch, Phys. Rev. E **59**, R2539 (1999).
[26] M.K. Shimamura and T. Doguchi, Phys. Rev. E **64**, 020801 (2001).

[27] K. Alim and E. Frey, Phys. Rev. Lett. **99**, 198102 (2007).
[28] M. Bohr and D.W. Heermann, J. Chem. Phys. **132**, 044904 (2010).
[29] P. Calabrese, A. Pelissetto, and E. Vicari, J. Chem. Phys. **116**, 8191 (2002).
[30] T. Sakaue, Phys. Rev. Lett. **106**, 167802 (2011).
[31] Y. Jung, C. Jeon, J. Kim, H. Jeong, S. Jun, and B.-Y. Ha, Soft Matter **8**, 2095 (2012).
[32] A. Rosa, E. Orlandini, L. Tubiana, and C. Micheletti, Macromolecules **44**, 8668 (2011).
[33] J. Shin, A. G. Cherstvy, and R. Metzler, New J. Phys. **16**, 053047 (2014).
[34] P. Cluzel, A. Lebrun, C. Heller, R. Lavery, J.-L. Viovy, D. Chatenay, and F. Caron, Science **271**, 792 (1996).
[35] H. Yamaguchi, K. Kubota and A. Harada, Nucleic Acids Symp. Ser., 229 (2000).
[36] Y.L. Lyubchenko, L.S. Shlyakhtenko, M. Binus, C. Gaillard, and F. Strauss, Nucleic Acids Res. **30**, 4902 (2002).
[37] J.C. Wang, Ann. Rev. Biochem. **54**, 665 (1985).
[38] J.J. Champoux, Ann. Rev. Biochem. **70**, 369 (2001).
[39] M.A. Krasnow and N.R. Cozzarelli, J. Biol. Chem. **257**, 2681 (1982).
[40] R. L. Duda, Cell **94**, 55 (1998).
[41] H.-X. Zhou, J. Am. Chem. Soc. **125**, 9280 (2003).
[42] R. Metzler, A. Hanke, P.G. Dommersnes, Y. Kantor, and M. Kardar. Phys. Rev. Lett. **88**, 188101 (2002).
[43] R. Metzler, Y. Kantor, and M. Kardar, Phys. Rev. E **66**, 022102 (2002).
[44] E. Ercolini, F. Valle, J. Adamcik, R. Metzler, P. de los Rios, J. Roca, and G. Dietler, Phys. Rev. Lett. **98**, 058102 (2007)
[45] W.R. Wikoff, L. Liljas, R.L. Duda, H. Tsuruta, R.W. Hendrix, and J.E. Johnson, Science **289**, 2129 (2000).
[46] J.W. Blankenship and P.E. Dawson, J. Mol. Biol. **327**, 537 (2003).
[47] M. Bohn and D.W. Heermann, J. Chem. Phys. **132**, 044904 (2010).
[48] M. Bohn, Heermann, O. Lourenc, and C. Cordeiro, Macromolecules **43**, 2564 (2010).
[49] B. Duplantier, J. Stat. Phys. **54**, 581 (1989).
[50] L. Schäfer, C. von Ferber, U. Lehr, and B. Duplantier, Nucl. Phys. B **374**, 473 (1992).
[51] G. S. Grest, K. Kremer, and T. A. Witten, Macromolecules **20**, 1376 (1987).
[52] H. P. Hsu, W. Nadler, and P. Grassberger, Macromolecules **37**, 4658 (2004).
[53] K. Ohno and K. Binder, J. Chem. Phys. **95**, 5444 (1991).
[54] K. Shida, K. Ohno, M. Kimura, and Y. Kawazoe, J. Chem. Phys. **105**, 8929 (1996).
[55] C. von Ferber and Yu. Holovatch, Condens. Matter Phys. **5**, 8 (1995).
[56] C. von Ferber and Yu. Holovatch, Theor. Math. Phys. **109**, 1274 (1996).
[57] C. von Ferber and Yu. Holovatch, Phys. Rev. E **65**, 042801 (2002).
[58] P.G. de Gennes, *Scaling Concepts in Polymer Physics* (Cornell University Press, Ithaca, 1979).
[59] J. des Cloizeaux and G. Jannink, *Polymers in Solutions: Their Modelling and Structure* (Clarendon Press, Oxford, 1990).
[60] H. Zimm and W. H. Stockmayer, J. Chem. Phys. **17**, 1301 (1949).
[61] J.J. Prentis, J. Chem. Phys. **76**, 1574 (1982); J. Phys. A: Math. Gen. **17**, 1723 (1984).
[62] A. Baumgärtner, J. Chem. Phys. **76** 4275 (1982).
[63] A. Miyake and K.F. Freed, Macromolecules **16**, (1983) 1228; Macromolecules **17**, 678 (1984).
[64] J.L. Alessandrini and Carignano M.A., Macromolecules **25**, 1157 (1992).
[65] M. Bishop M, J.H.R. Clarke, and J.J. Freire, J. Chem. Phys. **98**, 3452 (1993).
[66] G. Wei, Macromolecules **30**, 2125 (1997).
[67] R.I. Dima and D. Thirumalai, J. Phys. Chem. B **108**, 6564 (2004); C. Hyeon, R.I. Dima, and D. Thirumalai, J. Chem. Phys. **125**, 194905 (2006).
[68] N. Rawat and P. Biswas, J. Chem. Phys. **131**, 165104 (2009).
[69] T. Hu, A. Y. Grosberg, and B. I. Shklovskii, Biophys. J. **90**, 2731 (2006).
[70] W. Kuhn, Kolloid-Z. **68**, 2 (1934); R.O. Herzog, R. Illig, and H. Kudar, Z. Physik. Chem. Abt.

A, **167**, 329 (1934); F. Perrin, J. Physiq. Radium, **7**, 1 (1936).
[71] J.A. Aronovitz and D.R. Nelson, J. Physique **47**, 1445 (1986).
[72] J. Rudnick and G. Gaspari, J. Phys. A **19**, L191 (1986); G. Gaspari, J. Rudnick, and A. Beldjenna, J. Phys. A **20**, 3393 (1987).
[73] G. Wei and B.E. Eichinger, J. Chem. Phys. **104** 9142 (1996).
[74] M. Behamou and G. Mahoux, J. Physique Lett. **46**, L689 (1985).
[75] C. Domb and F.T. Hioe, J. Chem. Phys. **51**, 1915 (1969).
[76] M. Bishop and C.J. Saltiel, J. Chem. Phys. **88**, 6594 (1988).
[77] J.D. Honeycutt and D. Thirumalai, J. Chem. Phys. **90**, 4542 (1988).
[78] F. Drube, K. Alim, G. Witz, G. Dietler, and E. Frey, Nano Lett. **10**, 1445 (2010).
[79] K. Solc and W.H. Stockmayer, J. Chem. Phys. **54**, 2756 (1971); K. Solc, J. Chem. Phys. **55**, 335 (1971).
[80] S.F. Edwards, Proc. Phys. Soc. Lond. **85**, 613 (1965); Proc. Phys. Soc. Lond. **88**, 265 (1965).